

Single Crystal Growth of $(\text{Mo}_x\text{Cr}_{1-x})\text{AlB}$ and $(\text{Mo}_x\text{W}_{1-x})\text{AlB}$ by Metal Al Solutions and Properties of the Crystals

Shigeru Okada, Kiyokata Iizumi,* Katsuya Kudaka,* Kunio Kudou, Masaaki Miyamoto,†
Yang Yu,‡ and Torsten Lundström§

Kanagawa University, Kanagawa, Yokohama 221, Japan; *Tokyo Institute of Polytechnics, Atugi 243-02, Japan; †Kokushikan University, Setagaya, Tokyo 154, Japan; ‡The Institute of Physical and Chemical Research (RIKEN), Wako, Saitama 351-01, Japan; and §Institute of Chemistry, University of Uppsala, P.O. Box 531, S-751 21 Uppsala, Sweden

Received January 21, 1997; accepted February 6, 1997

The single crystals of ternary borides MoAlB and WAlB , and quaternary borides $(\text{Mo}_x\text{ME}_{1-x})\text{AlB}$ ($\text{ME} = \text{Cr}, \text{W}, \text{V}, \text{Nb}, \text{Ta}$) were grown by the flux method using molten aluminium as a solvent. The as-growth MoAlB , WAlB , $(\text{Mo}_x\text{Cr}_{1-x})\text{AlB}$, and $(\text{Mo}_x\text{W}_{1-x})\text{AlB}$ single crystals were subjected to chemical analyses and measurements of unit cell parameters. The homogeneity range for the solid solutions of $(\text{Mo}_x\text{Cr}_{1-x})\text{AlB}$ and $(\text{Mo}_x\text{W}_{1-x})\text{AlB}$ crystals was studied by X-ray powder diffraction and chemical analyses. However, the crystals of the ternary boride VAlB , NbAlB , and TaAlB and the quaternary boride $(\text{Mo}_x\text{V}_{1-x})\text{AlB}$, $(\text{Mo}_x\text{Nb}_{1-x})\text{AlB}$, and $(\text{Mo}_x\text{Ta}_{1-x})\text{AlB}$ compounds were not obtained. Crystallographic data, crystal size, crystal morphology, Vickers microhardness and electrical resistivity, and oxidation resistivity heated in air of MoAlB , WAlB , and $(\text{Mo}_x\text{ME}_{1-x})\text{AlB}$ ($\text{ME} = \text{Cr}$ and W) crystals were studied.

© 1997 Academic Press

INTRODUCTION

In the Mo-Al-B system, ternary phases $\text{Mo}_7\text{Al}_6\text{B}_7$ ($\text{MoAl}_{0.86}\text{B}$) (1) and MoAlB (UBC type) (space group $Cmcm$) (2) have been reported. The $\text{Mo}_7\text{Al}_6\text{B}_7$ phase has a composition very close to that of MoAlB but completely different unit cell parameters. In addition, in the W-Al-B system, it has been found that single crystals of a new compound WAlB (space group $Cmcm$) (3) and of the earlier known MoAlB can be grown by using the aluminium solution technique (4). Single crystal growth experiments have been performed in the Cr-Al-B and Va group (transition elements)- Al-B systems, however, ternary boride CrAlB , VAlB , NbAlB , and TaAlB phases were not reported (5–9). In previous work, we performed the preparation and structure analysis for the single crystals of MoAlB (4), WAlB (3), and $\text{Cr}_{1-x}\text{Mo}_x\text{AlB}$ ($x = 0.39$) (10). However, there is a little information about chemical and physical properties of MoAlB , $(\text{Mo}_x\text{ME}_{1-x})\text{AlB}$ ($\text{ME} = \text{Cr}$ and W), and WAlB

crystals. In this paper, we report experimental conditions for growing relatively large single crystals of the solid solution $(\text{Mo}_x\text{ME}_{1-x})\text{AlB}$ ($\text{ME} = \text{Cr}$ and W) by the high-temperature aluminium solution. The homogeneity range for the solid solutions of $(\text{Mo}_x\text{Cr}_{1-x})\text{AlB}$ and $(\text{Mo}_x\text{W}_{1-x})\text{AlB}$ was examined by X-ray powder diffraction and chemical analysis. Crystallographic data, crystal size, crystal morphology, Vickers microhardness and electrical resistivity, and oxidation resistivity at high temperature in air of these crystals were studied.

EXPERIMENTAL DETAILS

Single crystal growth experiments were performed in the system of the solid solution $(\text{Mo}_x\text{ME}_{1-x})\text{AlB}$ ($\text{ME} = \text{Cr}, \text{W}, \text{V}, \text{Nb}, \text{Ta}$) using high-temperature aluminium solution. The purities of the starting materials were as follows: Cr powder (purity 99.9%), Mo powder (purity 99.9%), W powder (purity 99.9%), V chips (purity 99.6%), Nb powder (purity 99.9%), Ta powder (purity 99.9%), B powder (purity 99.6%), and Al chips (purity 99.6%). They were weighted at the atomic ratio of $(\text{B}/(\text{Mo}_x\text{ME}_{1-x})) = 1.0$ ($\text{ME} = \text{Cr}, \text{W}, \text{V}, \text{Nb}, \text{Ta}$), and mixed with Al chips in the weight ratio 1 : 15. The amount of Mo in the starting materials was fixed at 2.0 g throughout all the experiments (4). The mixture was placed in a dense alumina crucible. The crucible was inserted in a vertical electric furnace. Purified Ar gas was flowing in the furnace as a protecting atmosphere against oxidation. Figure 1 shows the schematic arrangement of the growth apparatus. The mixture was heated at a rate of 300°C h^{-1} and held at $1500\text{--}1650^\circ\text{C}$ for 5 h. The solution was cooled to 1000°C at a rate of 50°C h^{-1} and then quenched to room temperature. The crystals were separated from the solidified mixture by dissolving the excess Al with 6 mol dm^{-3} hydrochloric acid for 2 to 3 days. The typical growth procedure is presented in Table 1. Experimental conditions for the growth of the single

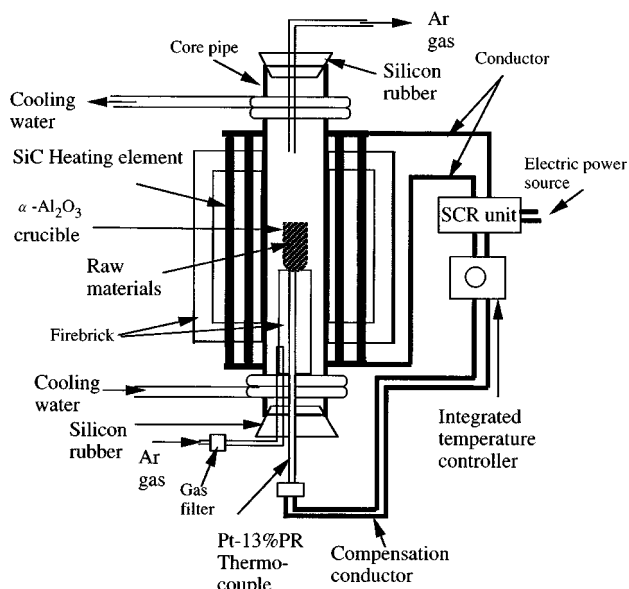
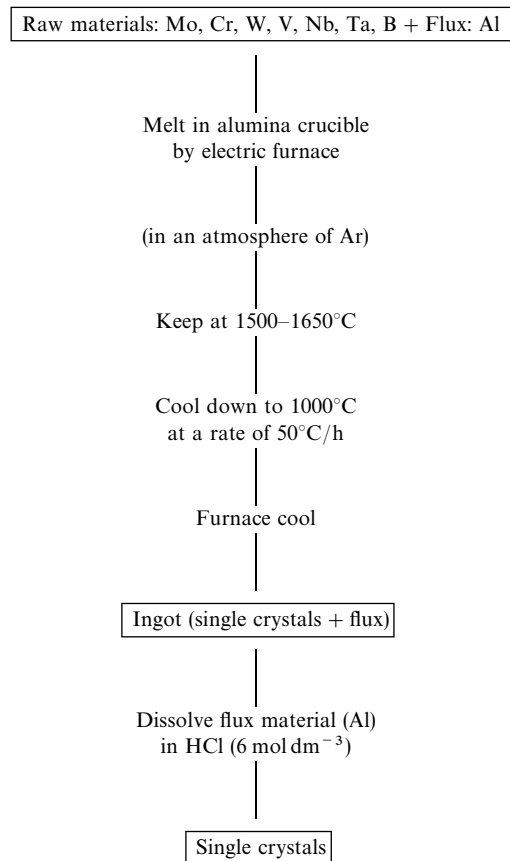


FIG. 1. Schematic arrangement of the growth apparatus.

crystals are shown in Table 2. Relatively large crystals of (Mo_xME_{1-x})AlB (*ME* = Cr and W) were selected under stereomicroscope for chemical analysis. The morphological properties and the impurity of the crystals were investigated by optical microscopy, a scanning electron microscope (SEM) (Hitachi, S-4000), an electron probe micro-analyzer (EPMA) (Jeol, JSM-35C), and an energy-dispersive detector (EDX) (Horiba, EMAX-2770). Chemical compositions were analyzed by EPMA and inductively coupled plasma (ICP) (Shimadzu, ICP-50) emission analysis (11). Phase analysis and determination of the unit cell parameters were performed using a powder X-ray diffractometer (XRD) (Rigaku, RINT-2500VHF) with monochromatic CuK α radiation ($\lambda = 0.154183$ nm) and a Guinier-Hägg focusing X-ray powder diffraction camera (XDC-1000 at Uppsala University, Sweden) with strictly monochromatic CuK α_1 radiation ($\lambda = 0.15405982$ nm) and semiconductor grade silicon as

TABLE 1
Preparations of MoAlB, WAlB, and (Mo_xME_{1-x})AlB (*ME* = Cr, W, V, Nb, Ta) Single Crystals by the Flux Method Using Molten Al as a Flux



an internal calibration standard (12). The unit cell parameters were determined by least-squares refinement using the program UNICELL (13). Thermogravimetric (TG) analysis and differential thermal analysis (DTA) were

TABLE 2
Typical Growth Conditions for the Single Crystals Obtained from Quarternary Mo–(Cr, W)–Al–B and Mo–(V, Nb, Ta)–Al–B Systems

Phases	Composition of the starting mixture in atomic ratio						B	Phases identified
	(Mo,	Cr,	W,	V,	Nb,	Ta): ^a		
MoAlB	1.0						1.0	MoAlB
WAlB			1.0				1.0	WAlB
(Mo _{0.65} Cr _{0.35})AlB	0.65	0.35					1.0	(Mo _{0.72} Cr _{0.28})AlB
(Mo _x W _{1-x})AlB	<i>X</i>		1 – <i>X</i>				1.0	(Mo _x W _{1-x})AlB (0 ≤ <i>X</i> ≤ 1.0)
(Mo _{0.9} V _{0.1})AlB	0.9			0.1			1.0	MoAlB, (Mo _x V _{1-x}) ₃ B ₄ , (Mo _x V _{1-x})B ₂
(Mo _{0.9} Nb _{0.1})AlB	0.9				0.1		1.0	MoAlB, (Mo _x Nb _{1-x})B ₂
(Mo _{0.9} Ta _{0.1})AlB	0.9					0.1	1.0	MoAlB, (Mo _x Ta _{1-x})B, (Mo _x Ta _{1-x}) ₃ B ₄

^a (Mo_xME_{1-x}): 2.0 g (*ME* = Cr, W, V, Nb, Ta), Al: 40.0 g. Soaking temperature, 1500°C; soaking time, 5 h.

performed between room temperature and 1200°C to study the oxidation resistivity of the crystals in air. A pulverized specimen of about 25 mg was heated at a rate of 10°C min⁻¹. The oxidation products were analyzed by a powder X-ray diffractometer. The Vickers microhardness of the as-grown MoAlB, (Mo_xME_{1-x})AlB (*ME* = Cr and W), and WAlB crystals were measured in several positions on *b* planes, at room temperature in air. A load of 50 g was applied for 15 s at about 5–8 points for each crystal, and the values obtained were averaged. The electrical resistivities of the crystals were measured by a direct-current four-probe technique at room temperature in air.

RESULTS AND DISCUSSION

*Characteristics and Crystal Morphology of MoAlB, WAlB, and (Mo_xME_{1-x})AlB (*ME* = Cr, W, V, Nb, Ta)*

Single crystals of ternary boride MoAlB and WAlB, and quaternary boride (Mo_xME_{1-x})AlB (*ME* = Cr, W, V, Nb, Ta) were grown by the flux method using molten aluminium as a solvent. It turned out that the quaternary phases (Mo_xCr_{1-x})AlB and (Mo_xW_{1-x})AlB were obtained in the Mo–Cr–Al–B and Mo–W–Al–B systems, respectively. The results of the phase analysis and the unit cell parameters of as-grown (Mo_xME_{1-x})AlB (*ME* = Cr and W) crystals are listed in Tables 3 and 4. Instead of any quaternary phase, however, only ternary MoAlB single crystals were obtained together with the ternary (Mo_xV_{1-x})₃B₄, (Mo_xV_{1-x})B₂, (Mo_xNb_{1-x})B₂, (Mo_xTa_{1-x})B, and (Mo_xTa_{1-x})₃B₄ phases in the Va elements (V, Nb, Ta)–Mo–Al–B systems. In our previous work, ternary VAlB, NbAlB, and TaAlB phases of the UBC-type structure were not obtained from the single crystal growth experiment in the V–Al–B, Nb–Al–B, and Ta–Al–B systems using the same crystal growth method (6–9). EDX and chemical analyses show that the compositions of the obtained MoAlB crystals in the Va elements–Mo–Al–B systems are close to the MoAlB composition (Table 3). This indicates that group Va elements have no solid solubility in MoAlB crystals, and

only group VIa elements form ternary and quaternary (Mo_xME_{1-x})AlB (*ME* = Cr and W) phases of the UBC-type structure. According to Yu and Lundström (10), from the crystal structure refinement and chemical analysis of the quaternary phases (Mo_xCr_{1-x})AlB, the chromium atoms were found to occupy the molybdenum atomic positions, and the chromium concentration was refined to *X* = 0.39. It is reported that the *X* values corresponding to the homogeneity range in (Mo_xCr_{1-x})AlB is about 0 ≤ *X* ≤ 0.4. The crystal structure of (Mo_xCr_{1-x})AlB is illustrated in Fig. 2 (10). The structure is conveniently described in terms of the trigonal prismatic arrangement of VIa transition metal atoms (Cr and Mo) surrounding each boron atom. The aluminium atoms form strongly puckered metal layers interleaved between the *ME* double layers, and the boron atoms form zigzag chains in the *z* direction.

On the other hand, in the (Mo_xW_{1-x})AlB system, considering the similarities in atomic radius of molybdenum and tungsten (14), an attempt was carried out to grow single crystals of (Mo_xW_{1-x})AlB in the Mo–W–Al–B system with the same crystal growth experiments as those in the Mo–Cr–Al–B system. The results are presented in Table 4, which indicate that tungsten atoms have solid solubility in MoAlB. This means that the *X* values corresponding to the homogeneity range in (Mo_xW_{1-x})AlB are 0 ≤ *X* ≤ 1.0.

(Mo_xW_{1-x})AlB single crystals, have silver color and metallic luster, were generally obtained as thick platelets with large *b* planes (Fig. 3a) and needle-like rectangles extending in the *c* axis direction (Fig. 3b). The largest crystals prepared have maximum dimensions of about 0.3 × 7.0 × 9.3 mm. (Mo_xCr_{1-x})AlB single crystals of needle-like rectangles with maximum dimensions of 1.0 × 1.0 × 6.4 mm with silver metallic luster, as shown in Fig. 4, were extracted from the solution.

Properties

The DTA-TG curves in air for MoAlB, WAlB, (Mo_{0.75}W_{0.25})AlB, (Mo_{0.5}W_{0.5})AlB, and (Mo_{0.8}Cr_{0.2})

TABLE 3
Representations of the (Mo_xCr_{1-x})AlB-Type Structure

Phases	Chemical compositions	Unit cell parameters				Ref.
		<i>a</i> (nm)	<i>b</i> (nm)	<i>c</i> (nm)	<i>V</i> (nm ³)	
MoAlB	—	0.32085(3)	1.3980(1)	0.31002(3)	0.13906	(10)
MoAlB	Mo _{1.09} Al _{1.04} B	0.3213(1)	1.3986(1)	0.3103(1)	0.1395(1)	This work
(Mo _{0.95} Cr _{0.05})AlB	(Mo _{0.93} Cr _{0.07})AlB	0.3207(1)	1.3980(1)	0.3099(1)	0.1390(1)	This work
(Mo _{0.90} Cr _{0.10})AlB	(Mo _{0.84} Cr _{0.16})AlB	0.3205(1)	1.3971(3)	0.3098(2)	0.1387(1)	This work
(Mo _{0.80} Cr _{0.20})AlB	(Mo _{0.80} Cr _{0.20})AlB	0.3196(1)	1.3968(3)	0.3089(1)	0.1379(1)	This work
(Mo _{0.65} Cr _{0.35})AlB	(Mo _{0.72} Cr _{0.28})AlB	0.3189(4)	1.3964(1)	0.3087(1)	0.1375(1)	This work
(Mo _x Cr _{1-x})AlB	(Mo _{0.61} Cr _{0.39})AlB	0.31702(6)	1.3948(2)	0.30743(4)	0.13594(6)	(10)

TABLE 4
Representations of the $(\text{Mo}_x\text{W}_{1-x})\text{AlB}$ -Type Structure

Phases	Chemical compositions	Unit cell parameters				Ref.
		<i>a</i> (nm)	<i>b</i> (nm)	<i>c</i> (nm)	<i>V</i> (nm ³)	
MoAlB	—	0.32085(3)	1.3980(1)	0.31002(3)	0.13906	(10)
MoAlB	$\text{Mo}_{1.09}\text{Al}_{1.04}\text{B}$	0.3213(1)	1.3986(1)	0.3103(1)	0.1395(1)	This work
$(\text{Mo}_{0.95}\text{W}_{0.05})\text{AlB}$	$(\text{Mo}_{0.97}\text{W}_{0.03})\text{AlB}$	0.3212(1)	1.3983(2)	0.3102(1)	0.1393(1)	This work
$(\text{Mo}_{0.75}\text{W}_{0.25})\text{AlB}$	$(\text{Mo}_{0.94}\text{W}_{0.06})\text{AlB}$	0.3211(1)	1.3972(4)	0.3104(2)	0.1393(2)	This work
$(\text{Mo}_{0.65}\text{W}_{0.35})\text{AlB}$	$(\text{Mo}_{0.68}\text{W}_{0.32})\text{AlB}$	0.3209(2)	1.3966(1)	0.3102(1)	0.1390(1)	This work
$(\text{Mo}_{0.50}\text{W}_{0.50})\text{AlB}$	$(\text{Mo}_{0.56}\text{W}_{0.44})\text{AlB}$	0.3210(2)	1.3963(5)	0.3105(2)	0.1392(2)	This work
$(\text{Mo}_{0.35}\text{W}_{0.65})\text{AlB}$	$(\text{Mo}_{0.42}\text{W}_{0.58})\text{AlB}$	0.3209(1)	1.3964(2)	0.3104(1)	0.1391(1)	This work
$(\text{Mo}_{0.25}\text{W}_{0.75})\text{AlB}$	$(\text{Mo}_{0.39}\text{W}_{0.61})\text{AlB}$	0.3205(2)	1.3965(2)	0.3109(2)	0.1392(2)	This work
WAlB	$\text{W}_{1.00}\text{Al}_{1.02}\text{B}$	0.3205(1)	1.3947(2)	0.3108(1)	0.1389(1)	(3)

AlB are shown in Figs. 5 and 6. According to TG curves, oxidation of the MoAlB, WAlB, $(\text{Mo}_{0.75}\text{W}_{0.25})\text{AlB}$, $(\text{Mo}_{0.5}\text{W}_{0.5})\text{AlB}$, and $(\text{Mo}_{0.8}\text{Cr}_{0.2})\text{AlB}$ compounds starts at about 730, 550, 715, 725, and 710°C, respectively. Weight gains of the samples after TG determination, heated to 1000°C in air, were found to be in the range of about 8.2 to 20.5 wt%. In contrast, the exothermic peaks of the DTA

curves were found at about 700 and 830°C for MoAlB, at about 970°C for WAlB, at about 740, 890, and 1020°C for $(\text{Mo}_{0.75}\text{W}_{0.25})\text{AlB}$, at about 980°C for $(\text{Mo}_{0.5}\text{W}_{0.5})\text{AlB}$, and at about 720 and 880°C for $(\text{Mo}_{0.8}\text{Cr}_{0.2})\text{AlB}$. The oxidation products were analyzed by a powder X-ray diffractometer at room temperature. The final oxidation products of MoAlB, WAlB, $(\text{Mo}_{0.75}\text{W}_{0.25})\text{AlB}$, and $(\text{Mo}_{0.5}\text{W}_{0.5})\text{AlB}$ crystals contain mixed phases of MoO_3 (orthorhombic), WO_3 (orthorhombic), $\text{Al}_5(\text{BO}_3)\text{O}_6$ (orthorhombic), $\text{Al}_2(\text{WO}_4)_3$ (orthorhombic), and $\text{Al}_{18}\text{B}_4\text{O}_{33}$ (orthorhombic). On the other hand, in $(\text{Mo}_{0.8}\text{Cr}_{0.2})\text{AlB}$ crystals, the identified oxidation products were found to be MoO_3 (orthorhombic), $\text{Al}_4\text{B}_2\text{O}_9$ (orthorhombic), $\text{Al}_{18}\text{B}_4\text{O}_{33}$ (orthorhombic), $\text{Al}_5(\text{BO}_3)\text{O}_6$ (orthorhombic), and CrBO_3 (rhombohedral) phases, respectively. In all cases, a B_2O_3 phase was not detected by powder X-ray diffraction; noncrystalline B_2O_3 was probably formed during the oxidation reaction. The exothermic peaks of the DTA curves are attributed to oxidation. On the oxidation resistivity of MoAlB, $(\text{Mo}_{0.75}\text{W}_{0.25})\text{AlB}$, $(\text{Mo}_{0.5}\text{W}_{0.5})\text{AlB}$, and $(\text{Mo}_{0.8}\text{Cr}_{0.2})\text{AlB}$ compounds showed relatively high thermochemical stability. Hence oxidation resistivity of WAlB is relatively low.

The Vickers microhardness of the as-grown MoAlB, WAlB, $(\text{Mo}_x\text{Cr}_{1-x})\text{AlB}$, and $(\text{Mo}_x\text{W}_{1-x})\text{AlB}$ crystals were measured in several directions on the *b* planes. The Vickers microhardness are presented in Table 5. As seen from Table 5, essentially, both ternary MoAlB and WAlB, and quaternary phases $(\text{Mo}_x\text{Cr}_{1-x})\text{AlB}$ and $(\text{Mo}_x\text{W}_{1-x})\text{AlB}$ reveal relatively high hardness. It is found that the microhardness values of MoAlB and $(\text{Mo}_x\text{Cr}_{1-x})\text{AlB}$ crystals, 9.8(5)–11.4(9) GPa, were comparatively lower than those of the WAlB, $(\text{Mo}_{0.56}\text{W}_{0.44})\text{AlB}$, and $(\text{Mo}_{0.39}\text{W}_{0.61})\text{AlB}$ phases. The microhardness value of MoAlB, WAlB, $(\text{Mo}_x\text{Cr}_{1-x})\text{AlB}$, and $(\text{Mo}_x\text{W}_{1-x})\text{AlB}$ crystals are not reported in the literature.

The electrical resistivity of as-grown crystals is listed in Table 6. As seen from Table 6, the electrical resistivity

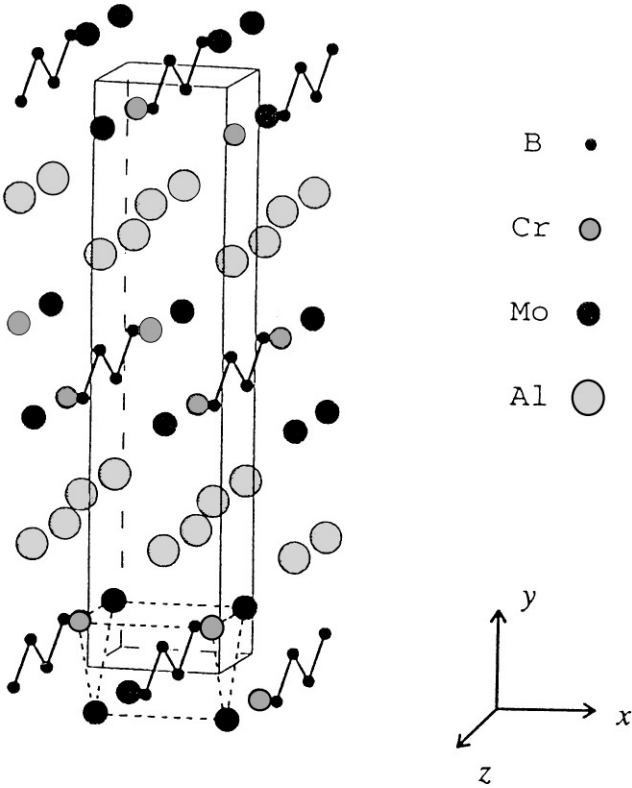


FIG. 2. The crystal structure of $\text{Mo}_{1-x}\text{Cr}_x\text{AlB}$. The boron bondings and one of the trigonal prisms are indicated. The molybdenum and chromium atoms are distributed randomly at the same atomic positions.

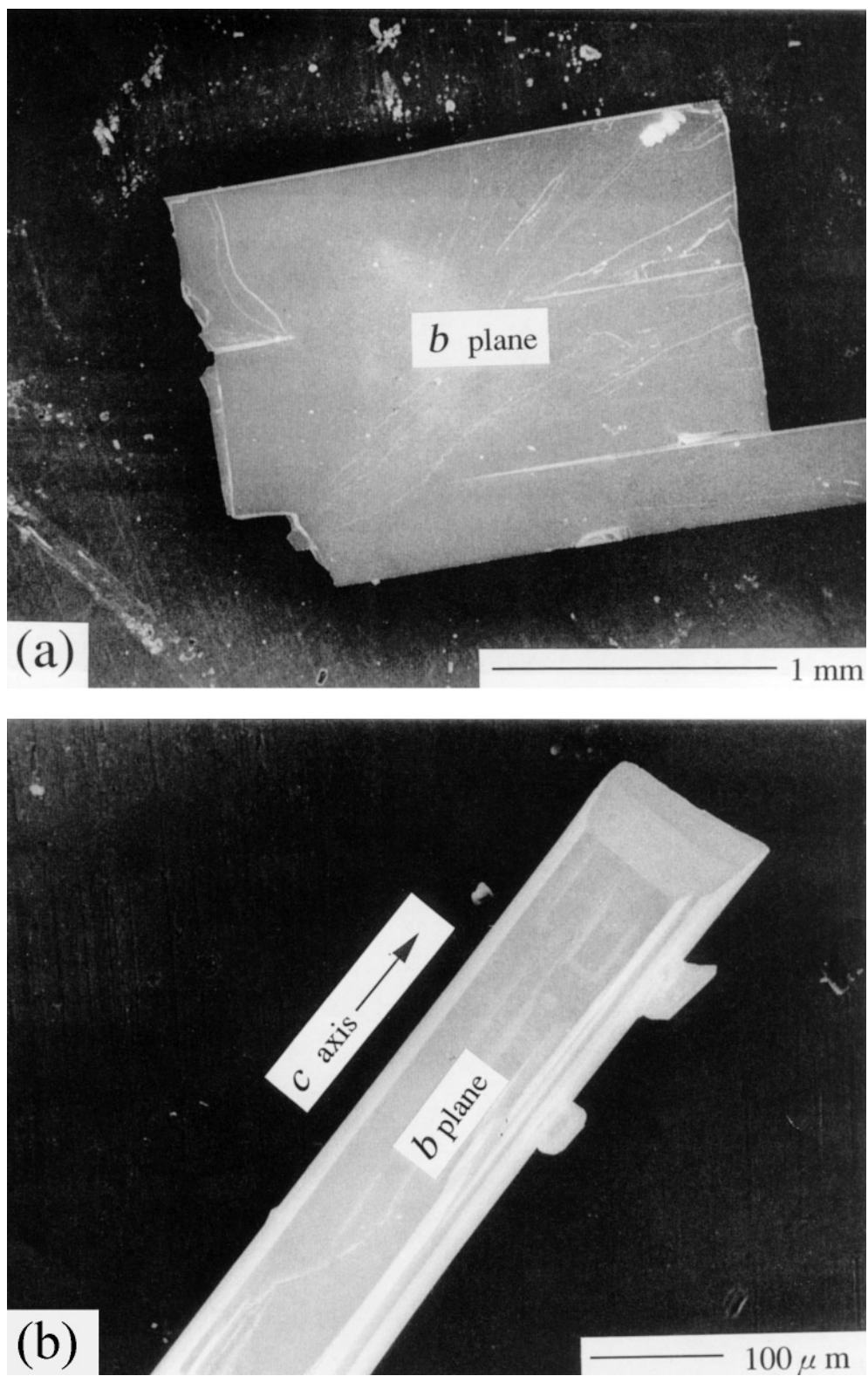
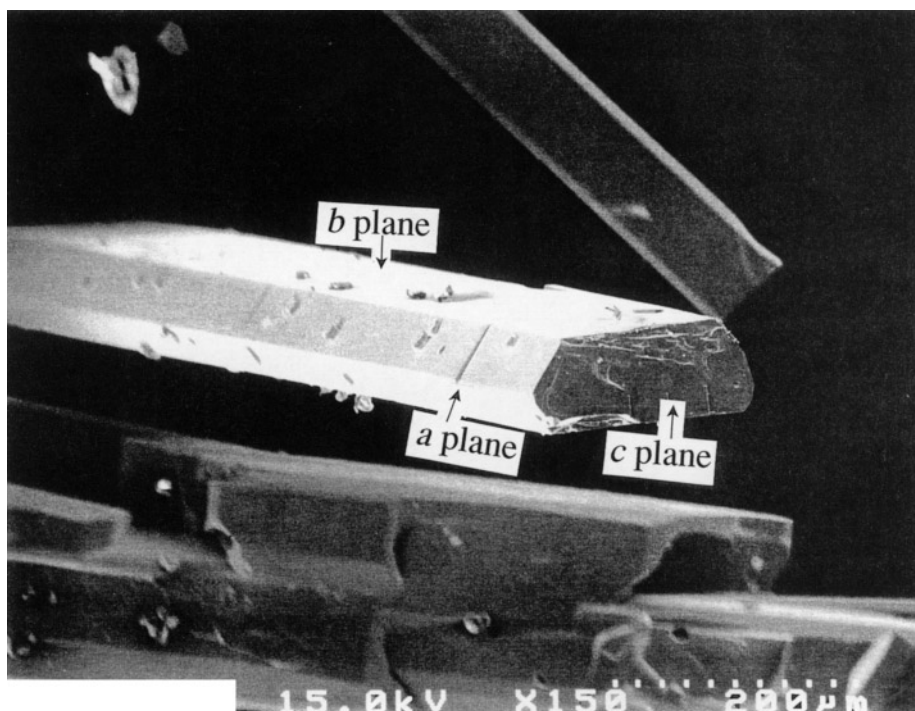


FIG. 3. SEM photographs of $(\text{Mo}_x\text{W}_{1-x})\text{AlB}$ single crystals.


 FIG. 4. SEM photograph of $(\text{Mo}_x\text{Cr}_{1-x})\text{AlB}$ single crystal.

values of MoAlB and $(\text{Mo}_x\text{Cr}_{1-x})\text{AlB}$ crystals were found to be lower than the values of the WAlB , $(\text{Mo}_{0.68}\text{W}_{0.32})\text{AlB}$, $(\text{Mo}_{0.56}\text{W}_{0.44})\text{AlB}$, and $(\text{Mo}_{0.39}\text{W}_{0.61})\text{AlB}$ phases by one

order of magnitude. The electrical resistivity value of MoAlB , WAlB , $(\text{Mo}_x\text{Cr}_{1-x})\text{AlB}$, and $(\text{Mo}_x\text{W}_{1-x})\text{AlB}$ crystals are not reported in the literature.

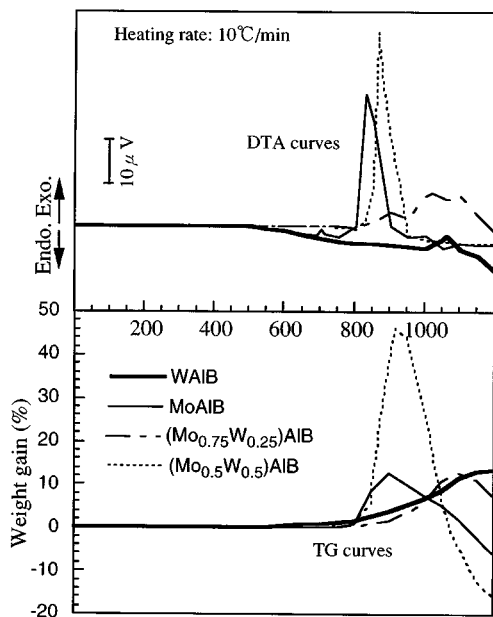
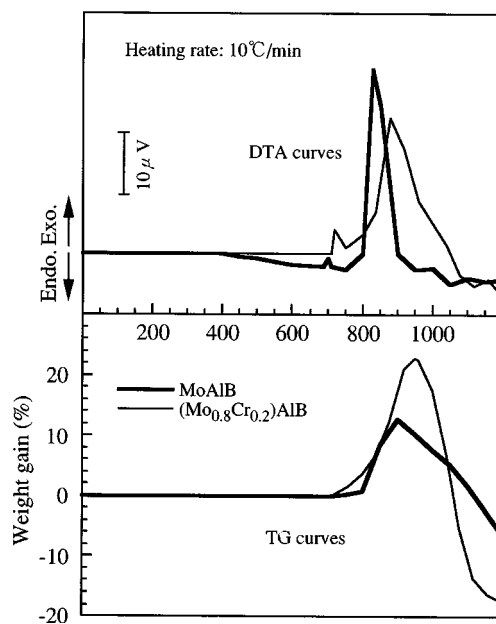

 FIG. 5. Differential thermal analysis and thermal gravimetric curves of MoAlB , WAlB , $(\text{Mo}_{0.75}\text{W}_{0.25})\text{AlB}$, $(\text{Mo}_{0.5}\text{W}_{0.5})\text{AlB}$ single crystals heated in air.

 FIG. 6. Differential thermal analysis and thermal gravimetric curves of MoAlB and $(\text{Mo}_{0.8}\text{Cr}_{0.2})\text{AlB}$ single crystals heated in air.

TABLE 5
Vickers Microhardness of MoAlB, WAlB, (Mo_xCr_{1-x})AlB,
and (Mo_xW_{1-x})AlB Single Crystals

Phases	Composition	Microhardness Hv (GPa)	Ref.
MoAlB	MoAlB	10.3(2)	This work
(Mo _{0.95} Cr _{0.05})AlB	(Mo _{0.93} Cr _{0.07})AlB	11.4(9)	This work
(Mo _{0.9} Cr _{0.1})AlB	(Mo _{0.84} Cr _{0.16})AlB	10.2(5)	This work
(Mo _{0.8} Cr _{0.2})AlB	(Mo _{0.80} Cr _{0.20})AlB	9.8(5)	This work
(Mo _{0.65} Cr _{0.35})AlB	(Mo _{0.72} Cr _{0.28})AlB	11.1(3)	This work
(Mo _{0.95} W _{0.05})AlB	(Mo _{0.97} W _{0.03})AlB	10.5(3)	This work
(Mo _{0.65} W _{0.35})AlB	(Mo _{0.68} W _{0.32})AlB	11.6(3)	This work
(Mo _{0.5} W _{0.5})AlB	(Mo _{0.56} W _{0.44})AlB	15.4(3)	This work
(Mo _{0.35} W _{0.65})AlB	(Mo _{0.39} W _{0.61})AlB	17.2(3)	This work
WAlB	WAlB	19.3(7)	This work

Note. Load, 50 g; load time, 15 s.

CONCLUSIONS

The single crystals of ternary boride MoAlB and WAlB, and quaternary boride (Mo_xME_{1-x})AlB (ME = Cr, W, V, Nb, Ta) have been grown by the flux method using molten aluminium as a solvent. The as-growth MoAlB, WAlB, (Mo_xCr_{1-x})AlB, and (Mo_xW_{1-x})AlB crystals were subjected to chemical analyses and measurements of unit cell parameters. In addition, measurements of microhardness, electrical resistivity, and oxidation resistivity in air at high temperature were carried out.

(1) Single crystals of MoAlB, WAlB, (Mo_xCr_{1-x})AlB, and (Mo_xW_{1-x})AlB were grown; the ternary boride VAlB, NbAlB, and TaAlB and the quaternary boride (Mo_xV_{1-x})AlB, (Mo_xNb_{1-x})AlB, and (Mo_xTa_{1-x})AlB

TABLE 6
Electrical Resistivity of MoAlB, WAlB, (Mo_xCr_{1-x})AlB, and
(Mo_xW_{1-x})AlB Single Crystals

Phases	Composition	Electrical resistivity ρ ($\mu\Omega$ cm)	Ref.
MoAlB	MoAlB	67.1	This work
(Mo _{0.95} Cr _{0.05})AlB	(Mo _{0.93} Cr _{0.07})AlB	43.6	This work
(Mo _{0.9} Cr _{0.1})AlB	(Mo _{0.84} Cr _{0.16})AlB	27.8	This work
(Mo _{0.8} Cr _{0.2})AlB	(Mo _{0.80} Cr _{0.20})AlB	22.5	This work
(Mo _{0.65} Cr _{0.35})AlB	(Mo _{0.72} Cr _{0.28})AlB	38.4	This work
(Mo _{0.95} W _{0.05})AlB	(Mo _{0.97} W _{0.03})AlB	91.2	This work
(Mo _{0.65} W _{0.35})AlB	(Mo _{0.68} W _{0.32})AlB	108.4	This work
(Mo _{0.5} W _{0.5})AlB	(Mo _{0.56} W _{0.44})AlB	302.6	This work
(Mo _{0.35} W _{0.65})AlB	(Mo _{0.39} W _{0.61})AlB	358.2	This work
WAlB	WAlB	243.6	This work

phases were not obtained from the single crystal growth experiment in the Mo–V–Al–B, Mo–Nb–Al–B, and Mo–Ta–Al–B systems.

(2) MoAlB, WAlB, (Mo_xCr_{1-x})AlB, and (Mo_xW_{1-x})AlB single crystals were generally obtained as thick platelets with large *b* planes and needle-like rectangles extending in the *c* axis direction. The largest crystals prepared have maximum dimensions of about $0.3 \times 7.0 \times 9.3$ mm.

(3) The tungsten atoms had solid solubility in MoAlB. The *X* values corresponding to the homogeneity range in (Mo_xW_{1-x})AlB are $0 \leq X \leq 1.0$. The chromium atoms were found to occupy the molybdenum atomic positions, and the chromium concentration was refined to *X* = 0.39. The homogeneity range in (Mo_xCr_x)AlB is about $0 \leq X \leq 0.4$.

(4) By means of TG-DTA between room temperature and 1000°C, the oxidation of MoAlB, WAlB, (Mo_{0.75}W_{0.25})AlB, (Mo_{0.5}W_{0.5})AlB, and (Mo_{0.8}Cr_{0.2})AlB compounds in air starts at about 730, 550, 715, 725, and 710°C, respectively, and final weight gains were found to be in the range from about 8.2 to 20.5 wt%. Mixed phases of MoO₃, WO₃, Al₅(BO₃)O₆, Al₂(WO₄)₃, Al₄B₂O₉, Al₁₈B₄O₃₃, and CrBO₃ were identified by XRD as resultant product.

(5) Average values of Vickers microhardness (Hv) and electrical resistivity (ρ) determined for MoAlB, (Mo_{0.95}Cr_{0.05})AlB, (Mo_{0.9}Cr_{0.1})AlB, (Mo_{0.8}Cr_{0.2})AlB, (Mo_{0.65}Cr_{0.35})AlB, (Mo_{0.95}W_{0.05})AlB, (Mo_{0.65}W_{0.35})AlB, (Mo_{0.5}W_{0.5})AlB, (Mo_{0.35}W_{0.65})AlB, and WAlB crystals are as follows:

MoAlB	Hv = 10.3(2) GPa, ρ = 67.1 $\mu\Omega$ cm
(Mo _{0.95} Cr _{0.05})AlB:	Hv = 11.4(9) GPa, ρ = 43.6 $\mu\Omega$ cm
(Mo _{0.9} Cr _{0.1})AlB:	Hv = 10.2(5) GPa, ρ = 27.8 $\mu\Omega$ cm
(Mo _{0.8} Cr _{0.2})AlB:	Hv = 9.8(5) GPa, ρ = 22.5 $\mu\Omega$ cm
(Mo _{0.65} Cr _{0.35})AlB:	Hv = 11.1(3) GPa, ρ = 38.4 $\mu\Omega$ cm
(Mo _{0.95} W _{0.05})AlB:	Hv = 10.5(3) GPa, ρ = 91.2 $\mu\Omega$ cm
(Mo _{0.65} W _{0.35})AlB:	Hv = 11.6(5) GPa, ρ = 108.4 $\mu\Omega$ cm
(Mo _{0.5} W _{0.5})AlB:	Hv = 15.4(9) GPa, ρ = 302.6 $\mu\Omega$ cm
(Mo _{0.35} W _{0.65})AlB:	Hv = 17.2(8) GPa, ρ = 358.2 $\mu\Omega$ cm
WAlB:	Hv = 19.3(7) GPa, ρ = 243.6 $\mu\Omega$ cm

REFERENCES

1. W. Rieger, H. Nowotny, and Benesovsky, *Mh. Chem.* **96**, 844 (1965).
2. F. Halla and W. Thury, *Z. Anorg. Allg. Chem.* **249** (1992).
3. Y. Zhang, S. Okada, T. Atoda, T. Yababe, and I. Yasumori, *Yogyo-Kyokai-shi* **95**, 374 (1987).
4. S. Okada, T. Atoda, I. Higashi, and Y. Takahashi, *J. Mater. Sci.* **22**, 2993 (1987).
5. S. Okada, T. Atoda, and I. Higashi, *J. Less-Common Met.* **113**, 331 (1985).
6. S. Okada, K. Kudou, I. Higashi, and T. Lundström, "Proc. 11th Int. Symp. Boron, Borides and Related Compounds, Tsukuba, 1993." JJAP Series 10, pp. 132 (1994).
7. S. Okada and T. Lundström, *J. Crystal Growth* **129**, 543 (1993).

8. S. Okada, T. Atoda, and Y. Takahashi, *Nippon Kagaku Kaishi* **8**, 1535 (1985).
9. S. Okada, K. Kudou, I. Higashi, and T. Lundström, *J. Crystal Growth* **128**, 1120 (1993).
10. Y. Yu and T. Lundström, *J. Alloys Comp.* **226**, 5 (1995).
11. Y. Takahashi, I. Higashi, and S. Okada, *Bunseki Kagaku* **35**, 646 (1986).
12. S. Okada, K. Hamano, I. Higashi, T. Lundström, and L.-E. Tergenius, *Bull. Chem. Soc. Jpn.* **63**, 687 (1990).
13. B. I. Nöläng, Institute of Chemistry, University of Uppsala, P. O. Box 531, S-751 21 Uppsala, Sweden, private communication, 1990.
14. L. Pauling, "The Nature of the Chemical Bond." Cornell Univ. Press, New York, 1940.